Transformation of Mechanical Performance and Corrosion Susceptibility of Al-Zn-Mg Alloy through Varied Flame Rectifications

Shuai Li [a,b*], Shuaizhe Ai [a], Dan Guo [b], Dejun Yan [c], Hao Lu [d], Guoshun Yang [e], Rongzheng Xu [f], Chuanqing Liao [g], Ningning Li [a] and Yonggang Jiang [c]

[a] *School of Mechanical Engineering, North China University of Water Resources and Electric Power, Zhengzhou, 450045, China.*
[b] *School of Materials Science and Engineering, Dalian University of Technology, Dalian, 116024, China.*
[c] *CSSC Huangpu Wenchong Shipbuilding Company Limited, Guangzhou, 510715, China.*
[d] *School of Materials Science and Engineering, Xi'an shiyou University, Xi' an 710065, China.*
[e] *Aerospace Engineering Equipment (Suzhou) Co. Ltd., Suzhou, 215004, China.*
[f] *School of Materials Science and Engineering, Shenyang Aerospace University, Shenyang, 110136, China.*
[g] *Shanghai Aerospace Equipments Manufactureer Co., Ltd., Shanghai 200245, China.*

Authors' contributions

This work was carried out in collaboration among all authors. Authors SL, DG and SA performed the experiments and wrote the manuscript. Authors DY and HL contributed to the conception and design of the study. Authors GY and RX perform the analysis with constructive discussions. Authors CL and NL played an important role in interpreting the results. Author YJ contributed to the conception and design of the study. All authors read and approved the final manuscript.

Original Research Article

_____

*Corresponding author: E-mail: lyctlishuai@163com;

ABSTRACT

The mechanical properties and corrosion performance of Al-Zn-Mg alloy through varied flame rectifications was studied based on the intergranular corrosion, exfoliation corrosion experiment. The results showed that the flame rectification accelerated the corrosion susceptibility of Al-Zn-Mg alloy. And the maximum intergranular corrosion depth are detected with the value of 89 μm after three time of flame rectification. The tensile strength of Al-Zn-Mg alloy increased to 383 MPa after one time of flame rectification in 300 °C. Then there is no significant change of tensile strength of Al-Zn-Mg alloy with the increase of flame rectification times. The change of corrosion resistance of Al-Zn-Mg alloy with varied flame rectifications is mainly associated with the transformation of precipitates and grains. There is a notable increase in the precipitation of phases within the grains after one time of flame rectification at 300°C. However, after two times of flame rectification, a phenomenon of "redissolution" of precipitated phases occurs. After three times of flame rectification, small-sized new grains appear at the grain boundaries of the elongated grains within the correction area, which is the result of incomplete recrystallization in the alloy.

Keywords: Al-Zn-Mg alloy; flame rectification; microstructure; mechanical properties; corrosion performance.

1. INTRODUCTION

Aluminum alloy has the characteristics of high linear thermal expansion coefficient and low yield strength, which will produce distortion after welding thermal cycling. There are many factors affecting welding distortion, such as local shrinkage (longitudinal contraction, transverse contraction and angular distortion), root gap, etc. [1]. The welding distortion of aluminum alloy workpiece is inevitably caused by uneven heating and cooling during welding. Generally speaking, the measures to control welding distortion can be divided into three categories: 1. Before welding, during the design stage of welding structure, welding deformations can be predicted using computational methods (such as numerical simulation techniques). Subsequently, measures such as optimizing structural design and positioning weld seams reasonably can be employed to "proactively" control welding deformations. 2. During welding, in the stage of welding manufacturing (assembly),"proactive" control of welding deformations can be achieved by controlling heat input, optimizing welding sequences, and utilizing external constraints and counter-deformation measures. 3. Post-weld correction (thermal correction or mechanical correction), which falls under the category of "passive" control methods, which may increase costs and energy consumption [2,3]. If the welding distortion can not be controlled within the permissible range by measures such as before welding and during welding, post-weld correction is required.

Post welding straightening methods include mechanical straightening method (cold straightening) and flame rectification (FR) method (heat straightening) [4-6]. Mechanical straightening method is to use hammer, press and other mechanical methods to produce new plastic distortion of welded structural parts to offset the deformation of welding. According to the characteristics of metallic materials expand when heated and contract when cooled, FR is heat in welded distortion area and then cool, so that the welded structural parts can produce anti-deformation and achieve the purpose of straightening welding distortion [7]. Mechanical straightening is generally suitable for small parts, and FR is mainly suitable for large structural parts. FR can be divided into spot heating, linear heating and triangle heating according to heating methods, as shown in Fig.1 [8]. Fig. 2 shows the schematic diagram of the principle of triangular FR [8]. The FR is often heated by oxygen-acetylene flame, whose maximum temperature can reach about 3200 °C. The distortion part is heated by moving the oxy-acetylene flame and then immediately water-cooled to reduce the welding deformation. Owing to its advantages of easy operation and flexibility, FR is widely used in the welding distortion production of steel structural parts [9,10]. With the increasing application of high-strength aluminum alloy in equipment manufacturing, FR process of aluminum alloy and its effect on the structural properties of aluminum alloy are gradually attracting extensive attention.

Jiang et al. [9] studied the effects of straightening temperature on the mechanical properties of 7020 aluminum alloy by FR. The results showed that the mechanical properties of the welded joint

have no change when the straightening temperature is 125 °C. When the temperature is higher than 225 °C, the tensile strength of the welded joint increases gradually. When the straightening temperature is higher than 325 °C, the range of softening zone becomes wider and the hardness decreases gradually. Therefore, it is recommended that the correction temperature of 7020 aluminum alloy should be lower than 325 °C. The temperature testing indicates that the temperature field of FR is an instantaneous field, and a stable temperature field cannot be attained. Furthermore, the temperature field generated during FR is susceptible to operational factors. At the same time, Avent et al. [11-13] also emphasized that "The process remains more of an art than a science". It can be seen that the FR method can not accurately analyze the reasons for the change of alloy properties. In order to better investigate the effects of FR parameters on the microstructure and properties of 7N01 aluminum alloy, Xiong et al. [10] studied the effects of FR temperature on the microstructure and mechanical properties of the joint of aluminum alloy for high-speed train with the help of Gleeble thermal simulation testing machine. The results showed that the hardness of the weld zone was not sensitive to the FR temperature. When the temperature is lower than 300 ℃, the hardness of 7N01 aluminum alloy base metal and heat affected zone decreases, while the hardness increases within 300-350℃. In consequence, the recommended FR temperature of 7N01 aluminum alloy is 300-400℃.
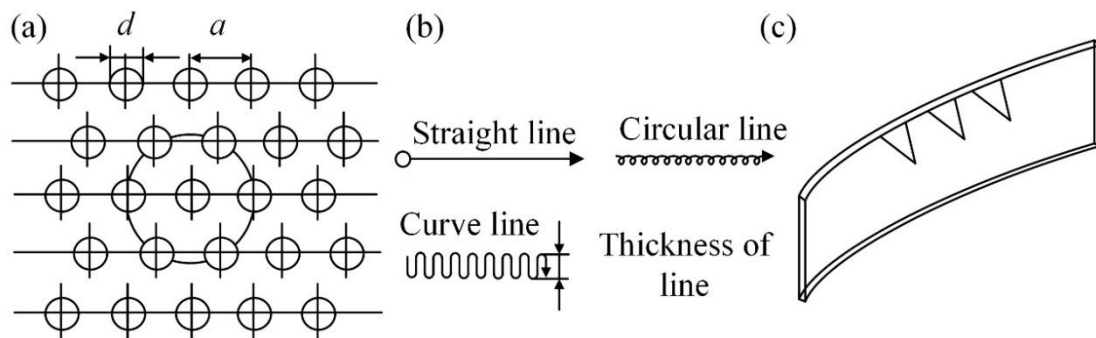

Fig. 1. The common heating methods for FR
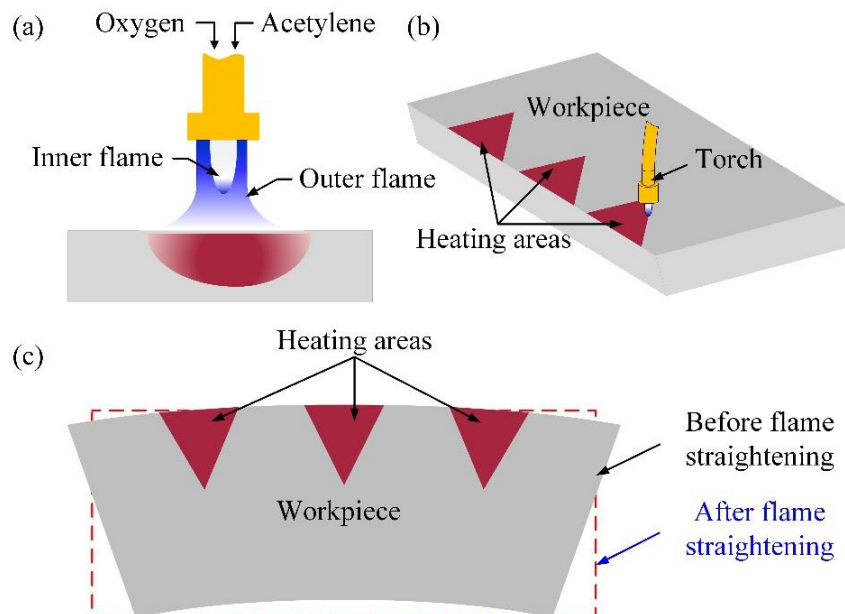*(a) spot heating; (b)linear heating; (c) triangle heating [8]*

Fig. 2. The schematic diagram of FR
(a) FR; (b) heat areas; (c) before and after flame rectification [8]

Based on the above research results, it is concluded that the investigation of FR of aluminum alloy mainly focused on the change of mechanical properties. Actually, the evaluation of corrosion resistance of aluminum alloy after FR is also important. Additionally, it is necessary to pay attention to the outside region apart from inside region of FR. In order to accurately evaluate the service reliability of the Al-4.5Zn-1.5Mg-T5(wt.%) aluminum alloy structural parts, the evolution of mechanical properties and corrosion susceptibility of the aluminum alloy inside and outside region of FR were studied after actual correction process in the paper. In the actual correction process, due to variations in welding deformations, frequently conduct multiple FR, with the number of FR typically not exceeding three.

2. EXPERIMENTAL PROCEDURE

2.1 Experimental Methods

The Al-4.5Zn-1.5Mg-T5(wt.%) extruded profile alloy was used during the FR process, the dimensions of Al-4.5Zn-1.5Mg-T5(wt.%) alloy are displayed in Fig. 3. The chemical composition of sample material is as shown in the Table 1. The route of oxygen and acetylene flame was set and the temperature was measured with tempilstik during FR process. The FR temperature is set at 300°C, with a heating time controlled within 2 minutes. The schematic diagram of sampling zones for the mechanical property and corrosion resistance evaluation was displayed in Fig. 4, the inside of triangle area is the flame rectification.

2.2 Microstructure Observation

The metallographic samples were rough ground and fine ground with SiC sandpaper to 2000#, followed by polishing with diamond paste with a particle size of 1.5 μm. After polishing, the specimens were etched with a mixed acid solution (2 mL HF + 3 mL HCl + 5 mL HNO$_3$ + 190 mL H$_2$O) for approximately 45 s. After etching, the specimens were immediately rinsed with water and then dried with a blow dryer. The metallographic structure of Al-4.5Zn-1.5Mg-T5(wt.%) alloy was observed using a Leica MEF4-type metallographic microscope. Scanning Electron Microscope (SEM) with the type of Zeiss Supra55 was used to investigate the micromorphology of corrosion resistance and fracture surfaces of Al-4.5Zn-1.5Mg-T5(wt.%) alloy.

2.3 Mechanical Performance

The testing equipment used was DNS100 universal tensile testing machine, with a tensile speed of 5 mm/min. Each measurement value represents the average of three parallel specimens. The dimension used for the thermal cycling is as shown in Fig. 5.
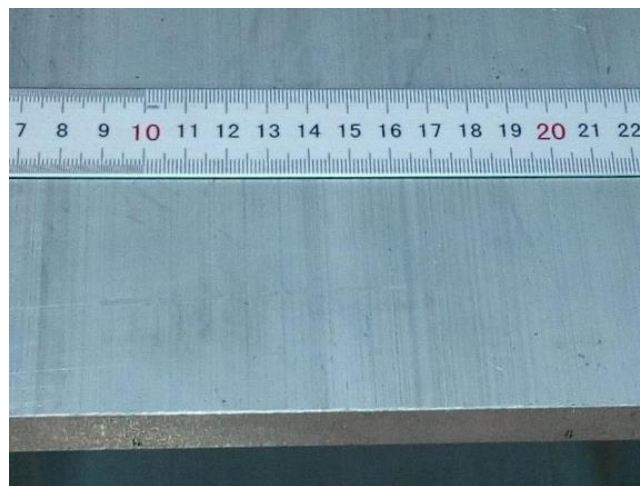

Fig. 3. The profile of as supplied Al-4.5Zn-1.5Mg alloy

Table 1. Chemical composition of Al-Zn-Mg alloy (wt.%)

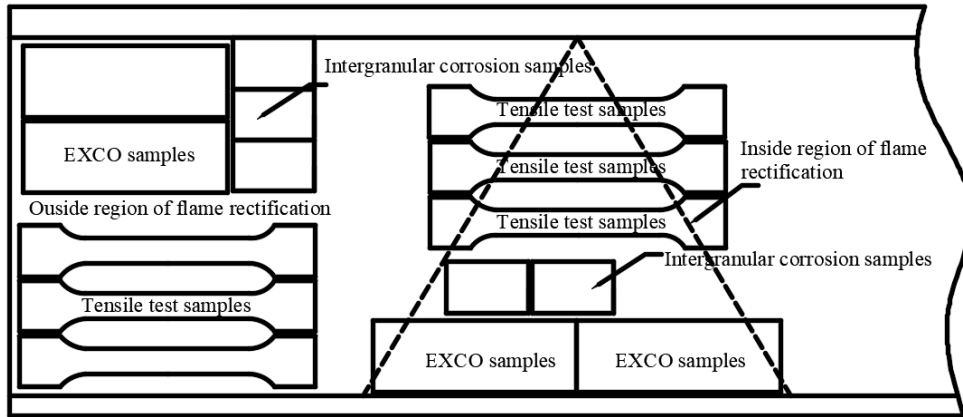| Materials	Zn	Mg	Mn	Cr	Zr	Fe	Cu	Ti	Si	Al
Al-4.5Zn-1.5Mg-T5	4.48	1.55	0.29	0.23	0.18	0.13	0.11	0.05	0.05	Bal.

Fig. 4. The schematic diagram of sampling zones of Al-4.5Zn-1.5Mg alloy
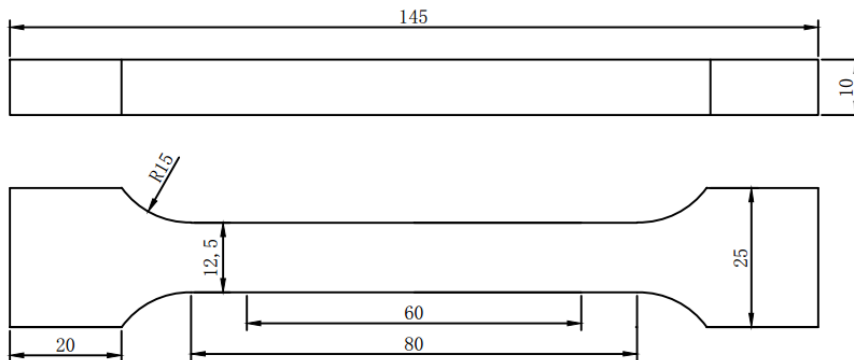

Fig. 5. Dimensions of repetitious FR samples for tensile test (Unit, mm)

2.4 Corrosion Test

The intergranular corrosion test was conducted according to the standared ASTM G110-92 and the samples with dimensions of 40 mm× 25 mm× 5 mm were extracted from the samples after flame rectification for intergranular corrosion (IGC) test [14]. The sample was polished to 1200# with SiC sandpaper and then rinsed with acetone to remove surface oil contamination before the experiment. The samples were immersed in a 10 wt.% NaOH solution for 5-15 minutes, then taken out and rinsed with deionized water. Then placed the sample in a 30 vol.% HNO$_3$ solution until the sample surfaces become bright. After rinsing with deionized water, the samples were dried and ready for further testing. The non-working surfaces of the samples were sealed with epoxy resin AB adhesive. The composition of the intergranular corrosion solution is as follows: 57 g of analytical grade NaCl, 10 mL of analytical grade H2O2, and finally diluted with deionized water to a total volume of 1 L. Use thermostatic water bath to maintain the soaking temperature within the range of 35±2 ℃. The intergranular corrosion samples were cut, ground, polished, and observed using an optical microscope (OM) to measure their corrosion depth.

The exfoliation corrosion (EXCO) test was conducted according to the standard ASTM G34-01[15]. The samples with dimensions of 40 mm× 30 mm× 5 mm were cut from the Al-4.5Zn-1.5Mg-T5(wt.%) alloy samples after different numbers of flame rectification for accelerated exfoliation corrosion test in water bath. The sample preparation process involves the following steps: sandpaper polishing, followed by cleaning with acetone, rinsing with deionized water, and then drying the samples. The composition of the corrosion solution is as follows: 4 M NaCl + 0.5 M KNO3 + 0.1 M HNO3. The PH of the solution is around 0.4, and the temperature of the corrosion solution is maintained at 25±2 ℃. The samples are immersed in the corrosion solution and taken out at regular intervals. The macroscopic corrosion

morphology of the sample surface is recorded using a camera, and the level of delamination corrosion is evaluated. The total immersion time is 48 h.

3. RESULTS AND DISCUSSION

3.1 Mechanical Property

Fig. 6 shows the changes of tensile strength and elongation of Al-4.5Zn-1.5Mg(wt.%) alloy in the straightening area under different FR times at 300 ℃. It can be seen that the mechanical properties in the straightening area changed significantly after different times in flame rectification at 300 ℃. The change of mechanical properties of the specimens with different numbers of flame rectification showed a trend of first increasing and then decreasing. The tensile strength increased to 383 MPa after one time of flame rectification, which increased by 9.42% than that of base metal. Then the tensile strength decreased with the increase of numbers of flame rectification, which is still close to that of base metal. The variation of elongation is opposite to that of tensile strength. After one time of flame rectification, the elongation decreased slightly, and gradually increased with the increasing of numbers of flame rectification.

The changes of tensile strength and elongation of Al-4.5Zn-1.5Mg(wt.%) alloy outside the straightening area under different numbers of flame rectification at 300 ℃ is displayed in Fig. 7. As can be seen from the figure, the variation trend of mechanical properties outside the straightening area is similar to that in the straightening area. The tensile strength generally presents a trend "first rising and then decreasing", and the elongation presents a trend of "first decreasing and then increasing".

Fig. 8 shows the fracture morphology of the specimens in the straightening area under different flame rectification times at 300℃, lots of dimples are observed, which displayed typical ductile fracture characteristics. The plastic deformation of specimens with different numbers of flame rectification can be evaluated by the dimple size of fractured specimens, namely the larger the dimple size, the better the plasticity of Al-4.5Zn-1.5Mg(wt.%) alloy. The fracture morphology of sample after one time of flame rectification is composed with fine dimples, as shown in Fig. 8b. Then dimple size of fractured specimen increased with the increase of number of flame rectification, as shown in Fig. 8c-d, which means the improvement of plasticity of flame rectification specimen. Fig. 9 shows the tensile fracture morphology of Al-4.5Zn-1.5Mg(wt.%) alloy outside the straightening area after different numbers of flame rectification at 300℃, which is similar with the Al-4.5Zn-1.5Mg(wt.%) alloy inside the straightening area after different numbers of flame rectification at 300℃.
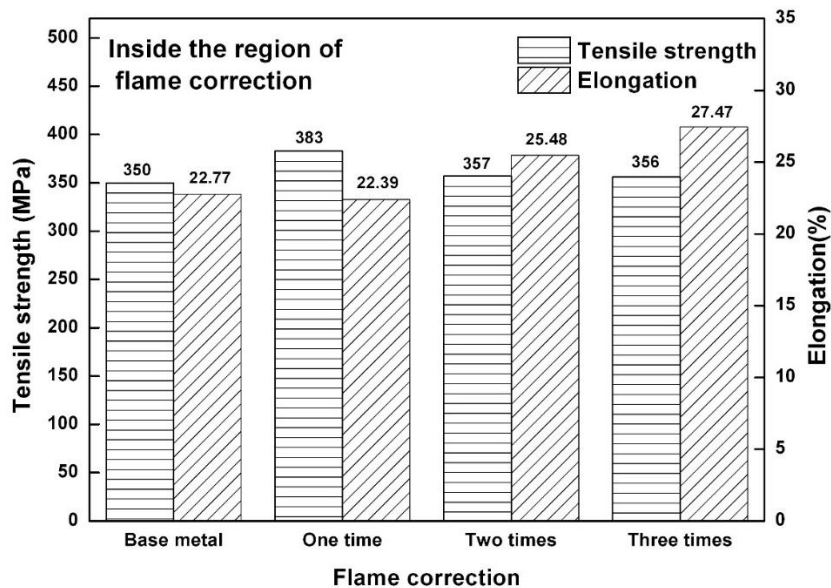

Fig. 6. Tensile strength and elongation of Al-4.5Zn-1.5Mg(wt.%) alloy inside the region of flame rectification in 300 °C
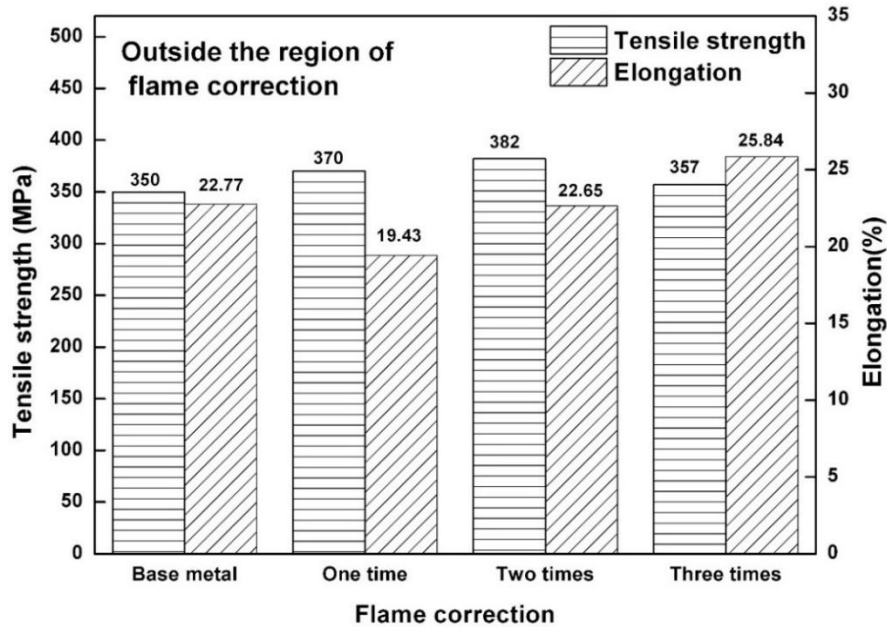
Fig. 7. Tensile strength and elongation of Al-4.5Zn-1.5Mg(wt.%) alloy outside the region of flame rectification in 300 °C
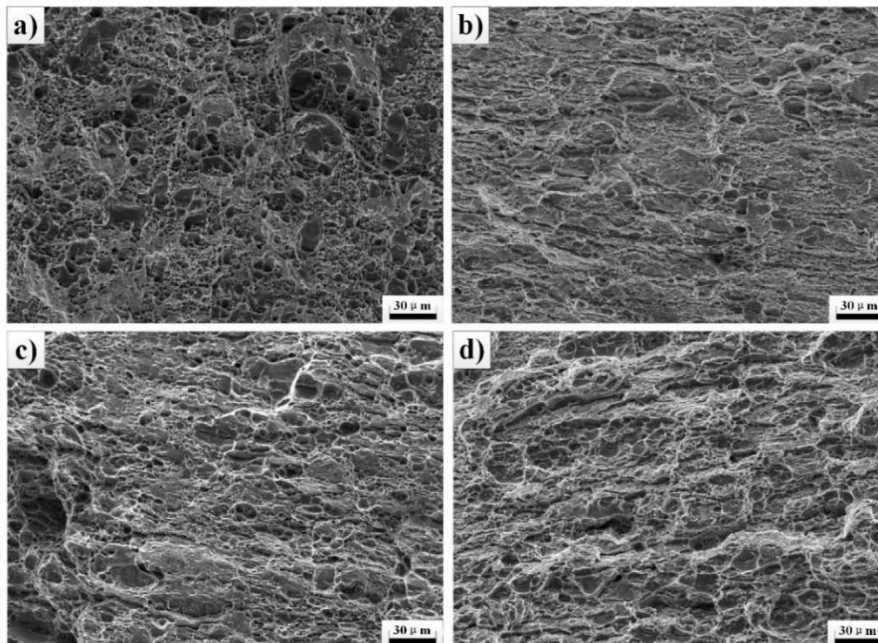

Fig. 8. SEM images of the tensile fractures of Al-4.5Zn-1.5Mg(wt.%) alloy inside the region of flame correction after different times of FR in 300 °C
(a) base metal, (b) one time, (c) two times (d) three times

According to the data of mechanical properties of heat treated specimens inside and outside the heat straightening area, it is concluded that no obvious deterioration of mechanical properties appeared after different numbers of flame rectification.

3.2 Corrosion Resistance

The Al-Zn-Mg alloys belongs to precipitation strengthening aluminum alloys, the change of mechanical performances and corrosion resistance are mainly associated with the

transformation of the precipitates [8,16,17]. According to the ranges of temperature for precipitation and dissolution of precipitate phases in typical Al-Zn-Mg alloys [8,16,17], the evolution of the precipitates of Al-4.5Zn-1.5Mg(wt.%) alloy will occur after different numbers of flame rectification, then resulted in the change of corrosion resistance.

Fig.10 shows the intergranular corrosion morphologies inside the straightening area after different numbers of flame rectification at 300 ℃. It can be seen from Fig.10 (a) that Al-4.5Zn-1.5Mg(wt.%) alloy has good intergranular corrosion resistance before flame rectification, and no obvious intergranular corrosion occurred. Then the intergranular corrosion occurred to different degrees for the samples with different numbers of flame rectification. The intergranular corrosion process of aluminum alloy belongs to electrochemical corrosion, which is mainly caused by the anodic dissolution of boundary precipitates (GBP) or grain boundary precipitate free zone (PFZ) [8]. Grain boundary is a place where defects, impurities and alloying elements are enriched, which is usually more active than in the grain, and GBP and PFZ have more negative potential values than the matrix, which making them act as anodes [8,17]. This leads to the formation of numerous corrosion microcells, resulting in intergranular corrosion phenomenon.

The intergranular corrosion susceptibility increased with the increasing of the flame rectification number, and the maximum intergranular corrosion depth of each sample is 76 μm, 86 μm and 89 μm, respectively. However, no intergranular corrosion morphology was observed in the samples outside the flame rectification area with different numbers of flame rectification.

Fig. 11 shows the macroscopic morphology of exfoliation corrosion of samples inside the straightening region after different numbers of flame rectification at 300 ℃. As can be seen from the Fig. 11a, the base metal lost its metallic luster and no obvious exfoliation corrosion phenomenon was observed. Then serious exfoliation corrosion occurred on the surface of the sample inside the straightening area after different numbers of flame rectification. The "bubbling," "peeling," and other exfoliation corrosion characteristics are obvious. The surface of specimens after flame rectification exhibited a delamination phenomenon, with layers forming and extending deeper into the interior. A large number of exfoliation corrosion products were observed after immersion corrosion testing. Additionally, the exfoliation corrosion showed typical heterogeneity, which was associated with the difference of thermal cycles during flame rectification.
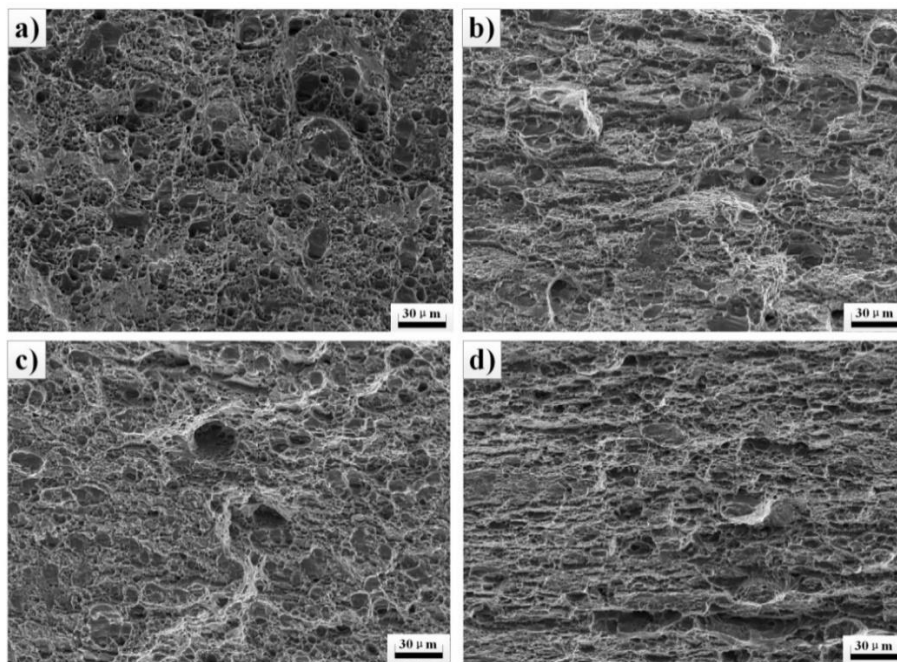

Fig. 9. SEM images of the tensile fractures of Al-4.5Zn-1.5Mg(wt.%) alloy outside the region of flame correction after different times of flame correction in 300°C
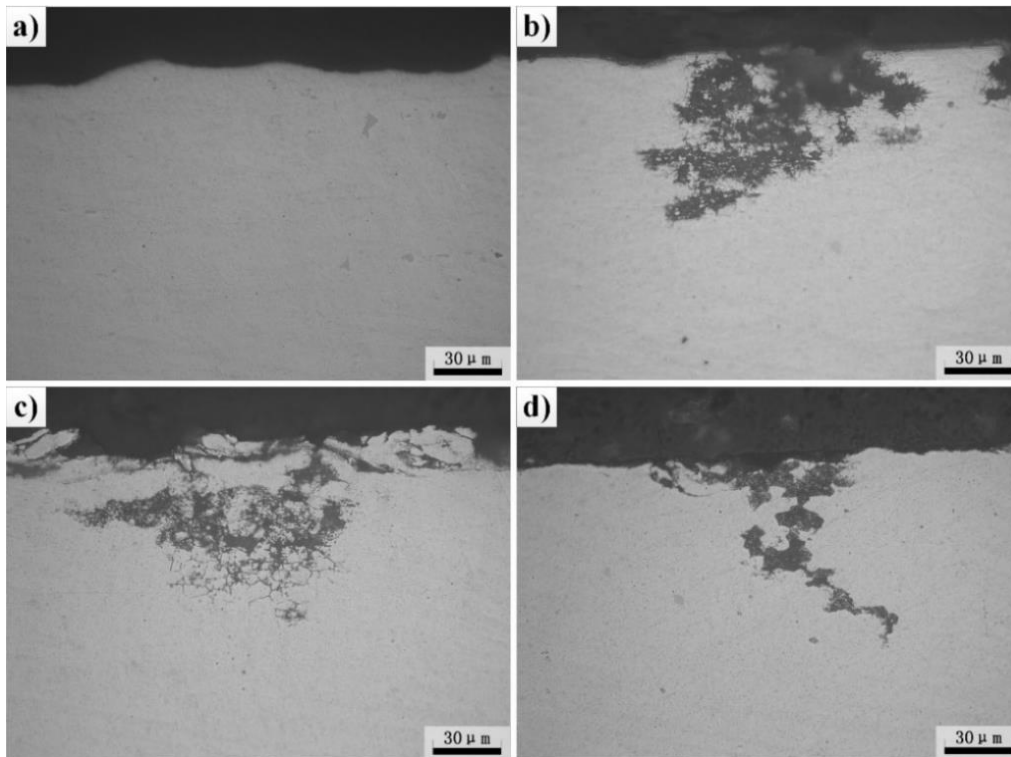*(a) base metal, (b) one time, (c) two times (d) three times*

Fig. 10. Intergranular corrosion micrographs of Al-4.5Zn-1.5Mg(wt.%) alloy inside the straightening region of flame correction after different times of flame correction in 300 °C
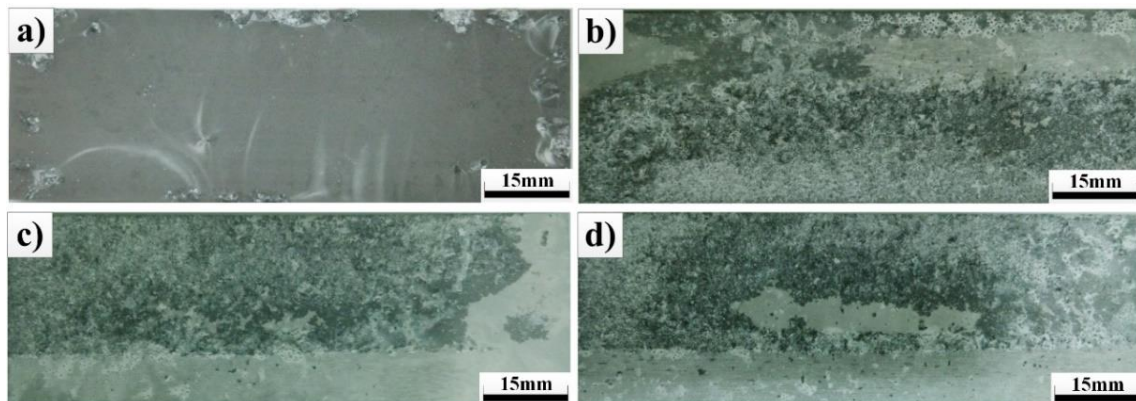*(a) base metal, (b) one time, (c) two times (d) three times*

Fig. 11. Surface morphology after exfoliation corrosion of Al-4.5Zn-1.5Mg(wt.%) alloy inside the region of flame correction after different times of flame correction in 300°C
(a) base metal, (b) one time, (c) two times (d) three times

Fig. 12 shows the macroscopic morphology of exfoliation corrosion of samples outside the straightening region after different numbers of flame rectification at 300 ℃. No exfoliation corrosion morphology on the surface of specimens was observed after one time or two times of flame rectification, which is similar to the base metal. However, serve exfoliation corrosion occurred for the sample after three times of flame rectification, which is likely associated with the

duration time in high temperature after three times of flame rectification.

Some exfoliation corrosion samples were cut and observed under scanning electron microscopy (SEM), and the results were shown in Fig 13. As can be seen from the figure, the base metal and samples inside the straightening region after different numbers of flame rectification showed various degrees of intergranular corrosion

cracking. Exfoliation corrosion of aluminum alloy is a special form of intergranular corrosion. The precipitated phase at grain boundaries has lower corrosion potential than that of matrix, so it is preferentially dissolved as anode, which makes the corrosion spread along the grain boundaries. After flame rectification, there are changes in the size, morphology, and distribution of the precipitated phases along the grain boundaries, making it easier for aluminum alloys to form continuous anodic corrosion pathways, thereby accelerating intergranular corrosion. At the surface grain boundaries, the volume of corrosion products is greater than the volume of metal consumed due to corrosion, leading to the generation of internal stress at the grain boundaries. This results in a "wedging effect," lifting the surface metal and causing delamination, ultimately leading to exfoliation. As a result, internal stress is generated at the grain boundaries, leading to the formation of a "wedging effect" that supports the surface metal and causes delamination, finally causes exfoliation. Therefore, the test results of exfoliation corrosion are generally consistent with those of intergranular corrosion. Xie et al. [18] analyzed the corrosion behavior of LY12CZ and 7075-T7351 high-strength aluminum alloys in exfoliation corrosion solution. They also considered that the formation stages of
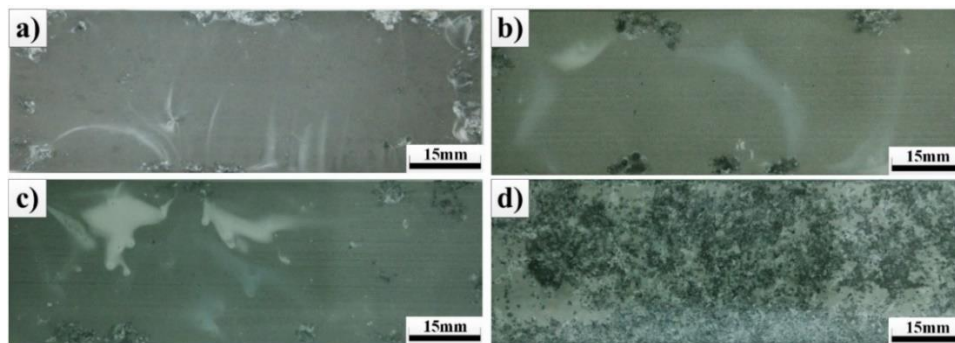

Fig.12. SEM morphology after exfoliation corrosion of Al-4.5Zn-1.5Mg(wt.%) alloy outside the straightening region after different times of flame correction in 300°C
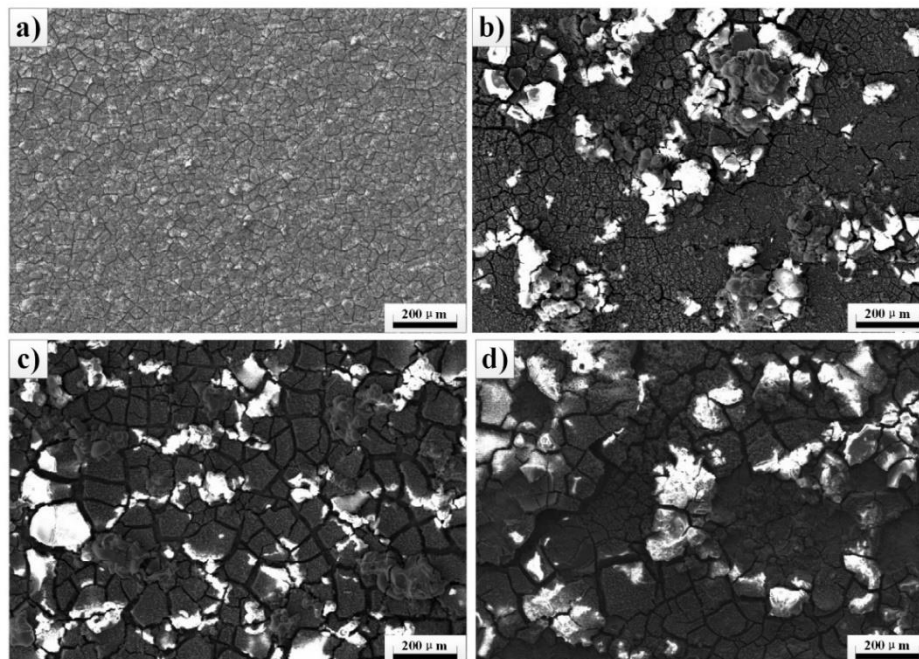(a) base metal, (b) one time, (c) two times (d) three times

Fig. 13. SEM morphology of Al-4.5Zn-1.5Mg (wt.%) alloy after exfoliation corrosion inside the straightening region of flame correction after different times of flame correction in 300℃
(a) base metal, (b) one time, (c) two times (d) three times
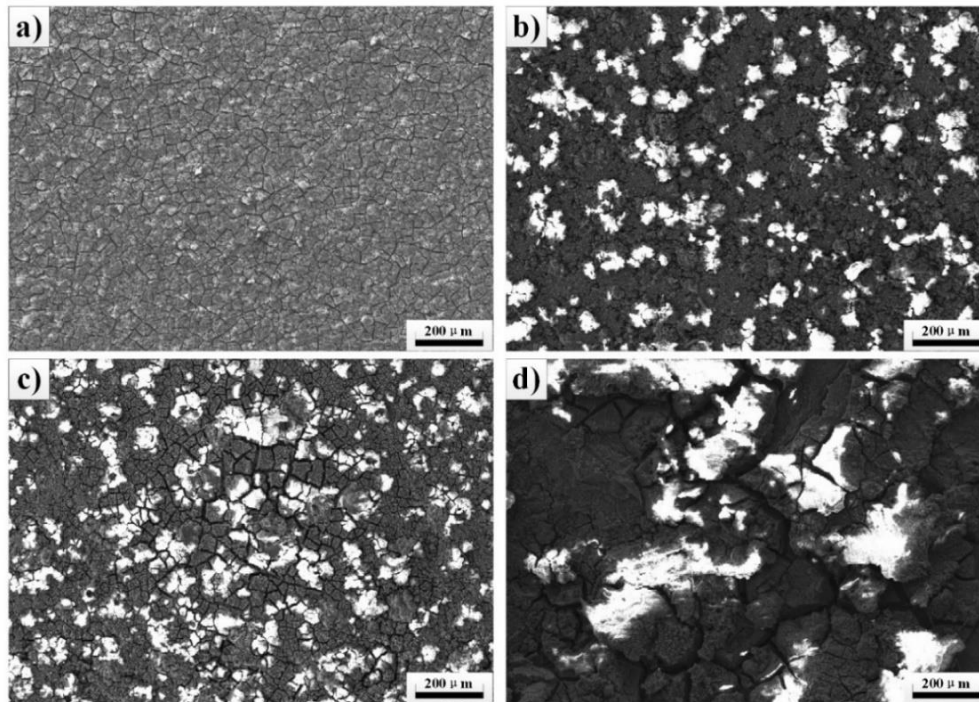
Fig.14. Surface morphology after exfoliation corrosion of Al-4.5Zn-1.5Mg(wt.%) alloy outside the region of flame correction after different times of flame correction in 300 ℃
(a) base metal, (b) one time, (c) two times (d) three times

exfoliation corrosion in high-strength aluminum alloys are as follows: it begins with pitting corrosion in the early stages and gradually progresses into exfoliation corrosion. Eventually, under the influence of internal stress, the corrosion propagates and deepens along grain boundaries, resulting in exfoliation phenomenon.

By comparing the microscopic morphology of exfoliation corrosion in the base metal and the samples after three times of flame rectification at 300 °C, it can be found that there are few exfoliation corrosion products on the surface of base metal while a large number of corrosion products are distributed on the surface of samples after flame rectification, as shown in Fig. 11a. The corrosion susceptibility increased with the increasing of times of flame rectification. Some areas have fallen off and separated from the surface of Al-4.5Zn-1.5Mg (wt.%) after three times of flame rectification.

Fig. 14 displayed the SEM morphology after exfoliation corrosion of the samples outside the straightening region after different numbers of flame rectification. The evolution of corrosion morphology of the specimens outside the straightening region is similar with the specimens inside the straightening region after different numbers of flame rectification and the exfoliation corrosion became severe with increasing the number of times of flame rectification.

Based on the results of intergranular corrosion and exfoliation corrosion tests, it can be concluded that the corrosion resistance of Al-4.5Zn-1.5Mg(wt.%) alloy deteriorates with increasing the number of times of flame rectification. For the Al-4.5Zn-1.5Mg(wt.%) alloy, the number of flame rectification at 300 ℃ should be less than two times.

4. CONCLUSION

The mechanical properties and corrosion performance of Al-Zn-Mg alloy through varied flame rectifications was studied based on the intergranular corrosion, exfoliation corrosion experiment. The results showed that the flame rectification accelerated the corrosion susceptibility of Al-Zn-Mg alloy. And the maximum intergranular corrosion depth are detected with the value of 89 μm after three time of flame rectification. The tensile strength of Al-Zn-Mg alloy increased to 383 MPa after one time of flame rectification in 300 °C. Then there is no

significant change of tensile strength of Al-Zn-Mg alloy with the increase of flame rectification times. The change of corrosion resistance of Al-Zn-Mg alloy with varied flame rectifications is mainly associated with the transformation of precipitates and grains. There is a notable increase in the precipitation of phases within the grains after one time of flame rectification at 300°C. However, after two times of flame rectification, a phenomenon of "redissolution" of precipitated phases occurs. After three times of flame rectification, small-sized new grains appear at the grain boundaries of the elongated grains within the correction area, which is the result of incomplete recrystallization in the alloy. In conclusion, when the flame temperature is 300°C, the most suitable number of flame rectification times for Al-Zn-Mg alloy material is less than two times.

ACKNOWLEDGEMENTS

COMPETING INTERESTS DISCLAIMER

Authors have declared that they have no known competing financial interests or non-financial interests or personal relationships that could have appeared to influence the work reported in this paper.

REFERENCES

1. Shuai Li, Honggang Dong, Xingxing Wang et al. Effect of repair welding on microstructure and mechanical properties of 7N01 aluminum alloy MIG welded Joint, J. Manuf. Process. 2020;54:80-88.
2. Deng D. FEM prediction of welding residual stress and distortion in carbon steel considering phase transformation effects. Mater. Des. 2009;30:359-366.
3. Deng D, Murakawa H. Prediction of welding distortion and residual stress in a thin plate butt-welded joint, Comp. Mater. Sci. 2008;43:353-365.
4. Deng D, Murakawa H, Liang W. Numerical simulation of welding distortion in large structures, Comput. Method. Appl. M. 2007;196:4613-4627.
5. Zhang Z, Jiang Z, Yu C. Automated flame rectification process planning system in shipbuilding based on artificial intelligence. Int. J. Adv. Manuf. Technol. 2006;30:1119-1125.
6. Lacalle R, Álvarez JA, Ferreño D, Portilla J, Ruiz E, Arroyo B, Gutiérrez-Solana F. Influence of the flame straightening process on microstructural, mechanical and fracture properties of S235 JR S460 ML and S690 QL structural steels, Exp. Mech. 2013;53:893-909.
7. Shuai Li, Honggang Dong, Peng Li, Su Chen. Effect of repetitious non-isothermal heat treatment on corrosion behavior of Al-Zn-Mg alloy, Corros. Sci. 2018;131:278-289.
8. Shuai Li, Microstructure,mechanical properties and corrosion behavior of Al-Zn-Mg alloy MIG welded joint, Dalian University of Technology, Dalian, China, 2018 D.S. Dissertation.
9. Jiang L, Wang Y, Liu A. Effect of flame straightening on microstructures and properties of welded joint of aluminium alloy for high-speed train, T Mater. Heat Treat. 2003;24:59-61.
10. Xiong Z. Effect mechanism of heat-straightening temperature on microstructure and properties of Aluminum alloy joint in high-speed trains. Harbin Institute of Technology, Harbin, China. M.S. Dissertation; 2014.
11. Avent RR. Heat-straightening of steel – Fact and fable, J. Struct. Eng. ASCE. 1989;115:2773-2793.
12. Avent RR, Fadous GM. Heat-straightening prototype damaged bridge girders, J. Struct. Eng. ASCE. 1989;115:1631-1649.
13. Avent RR, Mukai DJ. What you should know about heat straightening repair of damaged steel. Eng. J. AISC. 2001;38:27-49.
14. ASTM G110-92. Standard practice forevaluating intergranular corrosion resistance of heattreatable aluminum alloys by Immersion in Sodiumchloride+ hydrogen peroxide solution; 2009.
15. ASTM G34-01. Standard test method for exfoliation corrosion susceptibility in 2xxx and 7xxx Series Aluminum Alloys (EXCO Test); 2013.
16. Shuai Li, Dan Guo, Honggang Dong. Effect of flame rectification on corrosion property of Al-Zn-Mg alloy, Trans. Nonferrous Met. Soc. China. 2017;27:250-257.
17. Shuai Li, Honggang Dong, Lei Shi, Peng Li, Fei Ye. Corrosion behavior and mechanical properties of Al-Zn-Mg

aluminum alloy weld, Corros. Sci. 2017; 123:243-255.

18. Weijie Xie, Di Li, Yanling Hu, Baolan Guo. Statistical study of corrosion kinetics law for LY12CZ and 7075-T7351 aluminum alloy in EXCO solution, Acta Aeronaut. et Astronaut. Sinica. 1999; 20:34-38.

_____